

The STAT3 Inhibitor Galiellalactone Reduces IL6-Mediated AR Activity in Benign and Malignant Prostate Models



Florian Handle^{1,2}, Martin Pühr¹, Georg Schaefer³, Nicla Lorito¹, Julia Hoefler¹, Martina Gruber¹, Fabian Guggenberger¹, Frédéric R. Santer¹, Rute B. Marques⁴, Wytse M. van Weerden⁴, Frank Claessens², Holger H.H. Erb⁵, and Zoran Culig¹

Abstract

IL6/STAT3 signaling is associated with endocrine therapy resistance in prostate cancer, but therapies targeting this pathway in prostate cancer were unsuccessful in clinical trials so far. The mechanistic explanation for this phenomenon is currently unclear; however, IL6 has pleiotropic effects on a number of signaling pathways, including the androgen receptor (AR). Therefore, we investigated IL6-mediated AR activation in prostate cancer cell lines and *ex vivo* primary prostate tissue cultures in order to gain a better understanding on how to inhibit this process for future clinical trials. IL6 significantly increased androgen-dependent AR activity in LNCaP cells but importantly did not influence AR activity at castrate androgen levels. To identify the underlying mechanism, we investigated several signaling pathways but only found IL6-dependent changes in STAT3 signaling. Biochemical inhibition of STAT3 with

the small-molecule inhibitor galiellalactone significantly reduced AR activity in several prostate and breast cancer cell lines. We confirmed the efficacy of galiellalactone in primary tissue slice cultures from radical prostatectomy samples. Galiellalactone significantly reduced the expression of the AR target genes *PSA* ($P < 0.001$), *TMPRSS2* ($P < 0.001$), and *FKBP5* ($P = 0.003$) in benign tissue cultures ($n = 24$). However, a high heterogeneity in the response of the malignant samples was discovered, and only a subset of tissue samples (4 out of 10) had decreased PSA expression upon galiellalactone treatment. Taken together, this finding demonstrates that targeting the IL6/STAT3 pathway with galiellalactone is a viable option to decrease AR activity in prostate tissue that may be applied in a personalized medicine approach. *Mol Cancer Ther*; 17(12); 2722–31. ©2018 AACR.

Introduction

Patients suffering from castration-resistant prostate cancer (CRPC) still have a bad prognosis despite recent improvements in treatment options. The median life expectancy of CRPC patients is 16 to 18 months, and second-line therapies are able to increase the median overall survival by only a few months (1). The androgen receptor (AR) is reactivated in the majority of CRPC patients (2). However, the efficacy of subsequent AR-targeting/endocrine therapies is limited by the occurrence of preexisting resistance or rapid development of acquired resistance. In this

context, the second-generation antiandrogen enzalutamide increases the median overall survival of CRPC patients by only 2 to 5 months (3, 4). This demonstrates the urgent need to identify either novel drug targets or innovative ways to inhibit known key players such as the AR.

Interleukin-6 (IL6) is a paracrine and autocrine growth factor in prostate cancer and has been frequently associated with development of castration resistance (5–7). Circulating IL6 levels are increased in CRPC patients and IL6 is a predictive biomarker for poor prognosis (8). The canonical IL6 downstream mediator STAT3 is highly activated in metastatic samples from CRPC patients, and STAT3 activity is increased upon AR inhibition in LNCaP cells (9, 10). Furthermore, IL6 is a well-known activator of the AR and has been proposed to induce ligand-independent (outlaw) AR activity (11). The IL6/STAT3 axis is therefore a promising target for the treatment of advanced prostate cancer patients. In particular, the efficacy of endocrine therapy may be enhanced by disrupting the interaction between IL6 and AR signaling.

On the basis of this, several inhibitors for IL6 (i.e., siltuximab), JAK1/2 (i.e., ruxolitinib), STAT3 (i.e., galiellalactone), and other components of the IL6/STAT3 signaling cascade have previously been studied in prostate cancer (12). Galiellalactone induced apoptosis in stem cell–like ALDH-positive cells in two AR-negative prostate cancer cell lines and reduced the tumor growth as well as metastatic spread in an AR-negative xenograft model (13, 14). Besides prostate cancer, galiellalactone also inhibited the growth of triple-negative breast cancer cell lines (15). The

¹Division of Experimental Urology, Department of Urology, Medical University of Innsbruck, Innsbruck, Austria. ²Molecular Endocrinology Laboratory, Department of Cellular and Molecular Medicine, KU Leuven, Leuven, Belgium. ³Department of Pathology, Medical University of Innsbruck, Innsbruck, Austria. ⁴Department of Urology, Erasmus MC, University Medical Center Rotterdam, Rotterdam, the Netherlands. ⁵Department of Urology and Pediatric Urology, University Medical Center Mainz, Mainz, Germany.

Note: Supplementary data for this article are available at Molecular Cancer Therapeutics Online (<http://mct.aacrjournals.org/>).

H.H.H. Erb and Z. Culig share senior authorship of this article.

Corresponding Author: Zoran Culig, Medical University of Innsbruck, Anichstr. 35, A-6020 Innsbruck, Austria. Phone: 011-43-512-504-24717; Fax: 011-43-512-504-24817; E-mail: zoran.culig@i-med.ac.at

doi: 10.1158/1535-7163.MCT-18-0508

©2018 American Association for Cancer Research.

monoclonal anti-IL6 antibody siltuximab is approved for clinical use in multicentric Castleman disease and has been shown to successfully reduce IL6 signaling *in vitro* and *in vivo* in preclinical prostate cancer models (16–18). Surprisingly, siltuximab had no clinical benefit in chemotherapy pretreated CRPC patients in two phase II trials (19, 20). However, siltuximab monotherapy has not been tested in earlier stage patients, and it is possible that only certain patient subpopulations benefit from IL6 inhibition. Similarly, a clinical trial with the JAK1/2 inhibitor ruxolitinib in metastatic prostate cancer patients was terminated due to lack of response (12). This discrepancy between very promising preclinical studies and unsuccessful clinical trials demonstrates that there is an urgent need for more information about IL6/STAT3 signaling and in particular with regard to the interaction with AR signaling. Furthermore, alternative model systems that accurately reproduce the complex tumor microenvironment may be required to develop successful therapies against IL6 and its downstream mediators in prostate cancer.

Therefore, the aim of this study was to investigate the effect of IL6 on AR activation and evaluate the potential of inhibiting this process in primary patient tissue samples to overcome the limitations of cell culture model systems.

Materials and Methods

Reagents and chemicals

RPMI 1640 (product number: BE12-167F), DMEM low glucose (BE12-707F), DMEM/F12 (BE12-719F), sodium pyruvate (BE13-115E), and penicillin/streptomycin (17-602E) were purchased from Lonza. Glutamax (#35050-038) and phenol red free DMEM (A1443001) were purchased from Thermo Fisher Scientific. FCS (S181B-500) was purchased from Biowest. Nonessential amino acids (NEAA, M11-003) and charcoal/dextran (CSS)-treated FCS (SH30068.03) were obtained from GE Healthcare. Human IFN-gamma (I17001-100UG), insulin (#11376497001), and poly-D-lysine hydrobromide (P6407) were purchased from Sigma-Aldrich. The synthetic androgen R1881 was obtained from Organon, and the STAT3 inhibitor galiellalactone (sc-202165) was ordered from Santa Cruz. Recombinant human IL6 was purchased from R&D Systems (#206-IL-050), and recombinant LIF was purchased from Merck (LIF1010).

Cell culture

The cell lines LNCaP-FGC, VCaP, MCF7, and T-47D were obtained from ATCC. The DuCaP cell line was a kind gift from Prof. J. Schalken (Department of Urology, Radboud UMC, Nijmegen, the Netherlands). The identity of all cell lines was confirmed by short tandem repeat analysis. DuCaP cells were grown in RPMI 1640 supplemented with 10% FCS, 1% penicillin/streptomycin, and 1 × glutamax. MCF7 were cultivated in phenol red free DMEM supplemented with 10% FCS, 1% penicillin/streptomycin, 1 × NEAA, 1 mmol/L NaPyruvate, 10 µg/mL insulin, and 1 × glutamax. All other cell lines were cultured as recommended by the ATCC. Multiwell plates were precoated with poly-D-lysine hydrobromide for experiments with LNCaP cells. For steroid starvation experiments, the cells were cultivated in RPMI 1640 supplemented with 3% charcoal/dextran treated FCS (CSS-FCS), 1% penicillin/streptomycin, and 1 × glutamax. Benign primary basal epithelial cells (PrEP) were isolated as previously described (21) and differentiated into a more luminal phenotype by cul-

tivation in DMEM/F12 supplemented with 10% FCS, 1% penicillin/streptomycin, 1 × glutamax, and 10 nmol/L DHT for 7 days.

Ex vivo tissue slice cultures

The patient cohort consisted of 20 prostate cancer patients undergoing radical prostatectomy at the University Hospital of Innsbruck. The Ethics Committee of the Medical University of Innsbruck has approved the study (UN4837:317/4.7), and informed written consent was obtained from all patients. Small biopsy samples were taken from the explanted prostates by an expert pathologist from cancerous and adjacent benign areas. Correct assignment was confirmed histologically from thin slices of the punched core. The biopsy samples were immediately sliced into thin pieces with a razor blade and placed at the air-liquid interface on 70-µm cell strainers. The culture medium consisted of DMEM/F12 supplemented with 10% FCS, 1% penicillin/streptomycin, 1 × glutamax, 10 nmol/L DHT, and 5 ng/mL IL6.

Xenograft experiments

The patient-derived xenograft models and the PC346C cell line were selected from the Erasmus MC Rotterdam panel, including androgen-dependent (PC82, PC295, and PC310), castration-sensitive (PC346C), and castration-resistant (PC133, PC135, PC324, PC339, and PC374) models, which were established as described previously (22, 23). For the castration experiments, PC346C cells were cultured in prostate growth medium (DMEM/F12, 2% FCS, 1% ITS, 0.01% BSA, 10 ng/mL EGF, 100 ng/mL fibronectin, 20 µg/mL fetuine, 50 ng/mL cholera toxin, 0.1 mmol/L phosphoethanolamine, 0.6 ng/mL triiodothyronine, 500 ng/mL hydrocortisone, 0.1 nmol/L R1881, and 1% penicillin/streptomycin antibiotics). Cells (5 million in 100 µL PBS) were injected subcutaneously in the flank of male NMRI nude mice (NMRI-Foxn1nu, Taconic), and mice were castrated using standard surgical techniques when tumors reached ~150 mm³, as described previously (24). All experiments were approved by the Animal Experiments Committee under the Dutch Experiments on Animals Act, in adherence of the European Convention for Protection of Vertebrate Animals used for Experimental Purposes (Directive 2010/63/EU).

RNA isolation and RT-qPCR

Total RNA was isolated with the EXTRACTME TOTAL RNA KIT (DNA-Gdansk, EM09) according to the manufacturer's instructions. Tissue samples were homogenized with a 5-mm steel milling ball in TissueLyser II (Qiagen) at 30 Hz for 2 minutes. The RNA was reverse transcribed with the iScript Select cDNA Synthesis Kit (Bio-Rad, #1708897). RT-qPCR was performed on an ABI 7500 Fast system (Thermo Fisher Scientific) using the TaqMan Fast Advanced Master Mix (Thermo Fisher Scientific, #4444965). Custom primers were used at a concentration of 800 nmol/L each and FAM-TAMRA labeled probes at 150 nmol/L. The primer sequences were as follows: *HPRT1* (Fwd: GCTTTCCTTGCTCAGGCAGTA, Rev: GTCTGGCTTATATCCAACACTTCGT, Probe: TCAAGGTCGCAAGCTTGCTGGTGA AAAAGGA), *TBP* (Fwd: CACGAACCACGGCACTGATT, Rev: TTTTCTTGCTGCCAGTCTGGAC, Probe: TCTTCACTCTTGGCTCCCTGTGCACA), *PSA* (Fwd: GTCTGCGGCGGTGTTCTG, Rev: TGCCGACCCAGCAAGATC, Probe: CACAGCTGCCCACTGCATCAGGA), *AR* (Fwd: AGGATGCTCTACTTCGCCCC, Rev: ACTGGCTGTACATCCGGGAC, Probe: TGGTTTTCAATGAGTACCCGATGCACA), *SOCS3* (Fwd: TGATCCGCGACAGCTCG, Rev: TCCCAGACTGGTCTTGACG, Probe: CCAGCGCCACTTCTTCACGCTCA).

TaqMan Gene-Expression Assays from Thermo Fisher Scientific were used for *HMBS* (Hs00609297_m1), *TMPRSS2* (Hs01120965_m1), *FKBP5* (Hs01561006_m1), and *KRT8* (Hs01595539_g1). Thermo-cycling conditions were as recommended by the manufacturer. All expression data were normalized to the geometric mean of the three reference genes HPRT1, TBP, and HMBS.

Protein isolation and Western blotting

For all cell line experiments 10 to 50 μ g total protein was separated on NuPAGE Novex 4%–12% Bis-Tris Protein Gels (Thermo Fisher Scientific, #NP0335BOX) and transferred to 0.2- μ m nitrocellulose membranes (GE Healthcare, #10600001). Blocking of the membranes and antibody incubation was performed with 5% BSA in TBS-T. The primary antibodies were purchased from several companies: Merck Millipore: GAPDH (MAB374); Abcam: lamin-A (ab8980) and Cell Signaling Technology: AR (#5153), STAT3 (#9139), pSTAT3-Tyr705 (#9131), PTEN (#9188), p-AKT-Thr308 (#13038), p-AKT-Ser473 (#4060), AKT (#9272), pp44/42-Thr202/Tyr204 (#9106), p44/42 (#4695). Detection was performed on an Odyssey CLx near-infrared imager (LI-COR), and the protein expression was normalized to GAPDH. For the xenograft experiments, protein lysates (20 μ g in RIPA buffer) were run on 10% SDS-PAGE gels, blotted onto nitrocellulose membranes, stained with the pSTAT3-Tyr705 (#9145, Cell Signaling Technology) and STAT3 (ab32500, Abcam) antibodies and detected using SuperSignal West Femto Substrate (Thermo Fischer Scientific) on a C-DiGit Blot Scanner (LI-COR), as described previously (24). Nuclear fractionation was performed by vortexing the cells in a hypotonic detergent solution (1% Triton X-100, 0.1 mol/L citric acid) with protease and phosphatase inhibitors and subsequently pelleting the nuclei by centrifugation at 5000 RCF for 2 minutes. Protein expression in the nuclear fraction was normalized to lamin-A.

Proliferation measurements

Proliferation of stably transduced LNCaP cells expressing EmGFP-NLS was measured with the IncuCyte ZOOM live-cell imaging system (Essen BioScience) by counting the GFP labeled nuclei. Nuclei counts were \log_2 transformed, and the proliferation rate was measured once the cells maintained a stable growth rate.

Analysis of public transcriptome data sets

Transcriptome expression data of prostate cancer cell lines was analyzed with the Qlucore Omics Explorer 3.4 (Qlucore) from the geo database data sets GSE9633, GSE34211, GSE50936, GSE57083, and GSE36133 (25–28). Batch effects between the data sets were removed using the inbuilt factor elimination routine and visually verified by the clustering of the cell lines in principal component analysis plots. Glucocorticoid receptor (*GR*) expression data for undifferentiated PrEPs were obtained from previously published (29) transcriptome data from our group (GSE112686).

Statistical analysis

R (v3.4.2) was used for the statistical analysis. Student *t* test was used for the evaluation of statistical significance in all cell culture experiments, and the Wilcoxon signed rank test was used for the tissue slice culture experiments. For curve fitting of dose–response curves, nonlinear regression was used in GraphPad Prism 4. *P* values lower than 0.05 were considered significant and indicated

as follows: *, *P* < 0.05; **, *P* < 0.01; ***, *P* < 0.001. All experiments have been performed in at least three biological replicates unless noted otherwise.

Results

IL6 enhances the androgen-mediated activation of the AR

Since the unsuccessful clinical phase II trials with IL6 inhibition were performed in late-stage CRPC patients with prior endocrine therapies, we first wanted to clarify which treatment setting may benefit from IL6 inhibition. To this end, we assessed how IL6 affects the androgen response profile of the AR. We initially focused our experiments on the AR-positive prostate cancer cell line LNCaP because the majority of research on IL6-mediated AR activity has been performed with those cells. LNCaP cells were treated with increasing doses of the synthetic androgen R1881 in steroid-depleted medium for 72 hours in the presence and absence of 10 ng/mL IL6. Activity of the AR was evaluated by measuring the mRNA expression of the clinically relevant target genes PSA, *TMPRSS2*, and *FKBP5* by RT-qPCR (Fig. 1A and B). IL6 significantly enhanced the androgen-dependent AR activity on all target genes in the presence of moderate to high androgen concentrations, and the highest increase was observed at 1 nmol/L R1881. Interestingly, we did not observe any IL6-dependent increase in AR activity in the absence of R1881 or at low R1881 concentrations of 1 to 10 pmol/L (Fig. 1A and C). Of note, these findings demonstrate that IL6 potentiates the androgen-dependent activation of the AR but is not an androgen-independent AR outlaw activator in the context of endogenous target gene expression.

IL6-mediated AR activity is linked to induction of the STAT3 pathway

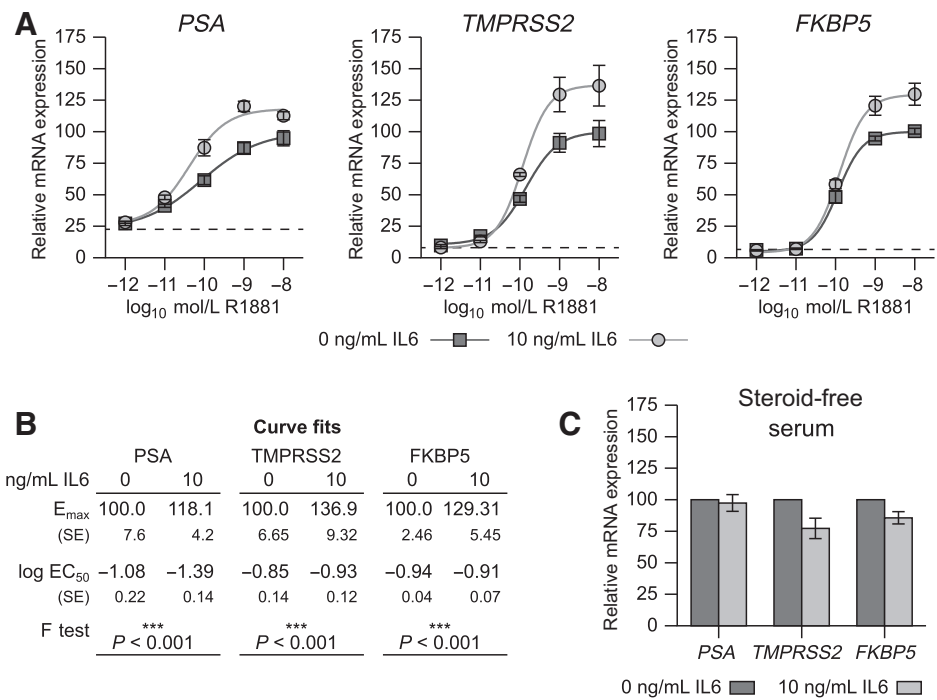
Our next aim was to elucidate which IL6 downstream pathway is responsible for modulation of AR activity. Previous publications have suggested changes in AR expression as well as several IL6 downstream pathways (STAT3, MAPK, and PI3K/AKT) as causes for IL6-mediated AR activity (30–34). To identify IL6-dependent changes, we measured the expression and activation of key components of these pathways in LNCaP cells after treatment with 10 ng/mL IL6 in the presence of 1 nmol/L R1881 (Fig. 2A). Importantly, we observed a strong induction of STAT3 phosphorylation as well as total STAT3 protein levels upon IL6 treatment. Due to the PTEN loss in LNCaP cells, we observed a strong basal activation of the PI3K/AKT pathway that was, however, unaffected by IL6 treatment. In addition, we did not detect any IL6-mediated MAPK activation at 72 hours of IL6 treatment. Subcellular localization of AR was unchanged by IL6, whereas STAT3 was significantly enriched in the nucleus (Fig. 2B). This demonstrates that the effect of IL6 is not mediated via MAPK or PI3K/AKT signaling in LNCaP cells and that AR protein expression and localization remains unchanged in the investigated cell line. Therefore, the effect of IL6 on AR activity is most likely mediated by STAT3, which may allow a more specific inhibition of this process compared with previous anti-IL6 treatment strategies.

STAT3 is highly activated in castration-resistant xenografts

To identify whether STAT3 inhibition is a promising approach for CRPC patients, we evaluated the activation level of STAT3 in a prostate cancer xenograft panel (Fig. 3A). We found high levels of phosphorylated STAT3 in all castration-resistant xenografts

Figure 1.

IL6 enhances the androgen-mediated activation of the AR. LNCaP cells were treated with the given concentration of the synthetic androgen R1881 in steroid-depleted medium for 72 hours in the presence or absence of 10 ng/mL IL6. AR activity was measured by RT-qPCR. Relative mRNA expression (A) and nonlinear curve fit (B) of the AR target genes *PSA* (*KLK3*), *TMPRSS2*, and *FKBP5*. The dashed line represents the basal expression without R1881/IL6. C, Effect of IL6 on AR activity in steroid-depleted medium without the addition of androgens.

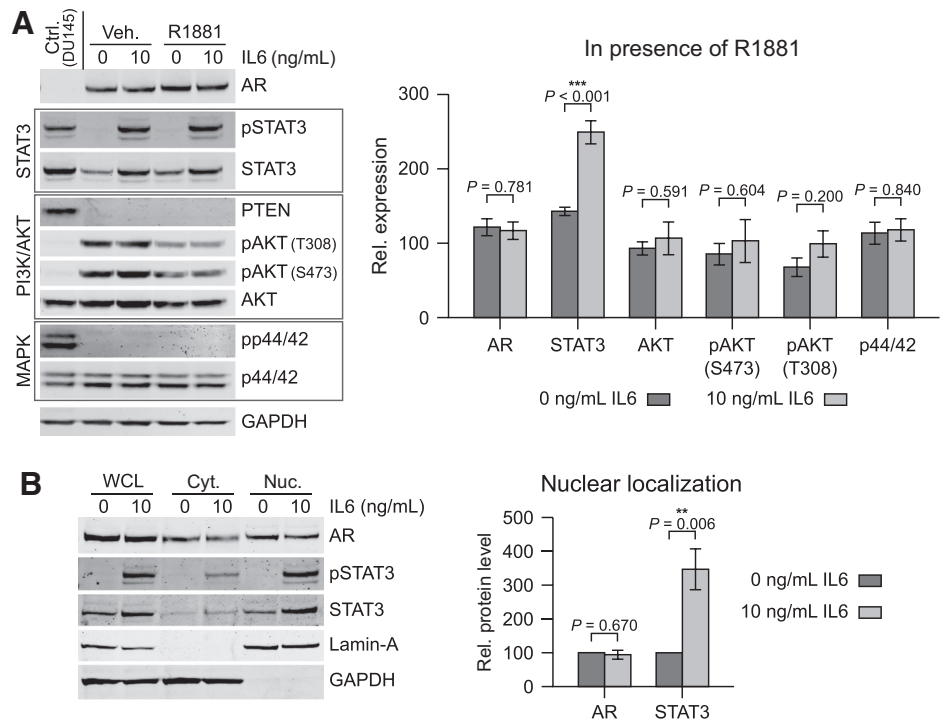


(PC133, PC135, PC324, PC339, and PC374) as well as in the androgen-responsive PC346C xenograft. In contrast, activation of STAT3 was very low in androgen-dependent xenografts (PC82, PC295, and PC310). In addition, we found increased STAT3 phosphorylation in androgen-responsive PC346C xenografts upon castration (Fig. 3B). Because STAT3 is activated in response to several stimuli, we tested whether the cytokines IFN-gamma

and LIF as well as bacterial endotoxin (LPS) are able to induce AR activity. All three compounds were able to induce expression of the STAT3 target gene *SOCS3* (Supplementary Fig. S1A). Interestingly, we observed a significant increase in PSA mRNA expression upon treatment with IFN-gamma, LIF, and LPS (Fig. 3C), which was similar in magnitude to IL6 treatment. However, in contrast to IL6 we did not observe any induction of *TMPRSS2* and

Figure 2.

IL6-mediated AR activity is linked to induction of the STAT3 pathway. LNCaP cells were treated with 1 nmol/L of R1881 in steroid-depleted medium for 72 hours in the presence or absence of 10 ng/mL IL6 before harvesting. A, Activation of IL6 downstream pathways and total AR levels were measured by Western blotting. B, Localization of STAT3 in the whole-cell lysate (WCL), cytoplasm (cyt.), and nucleus (nuc.) measured after subcellular fractionation by Western blotting.



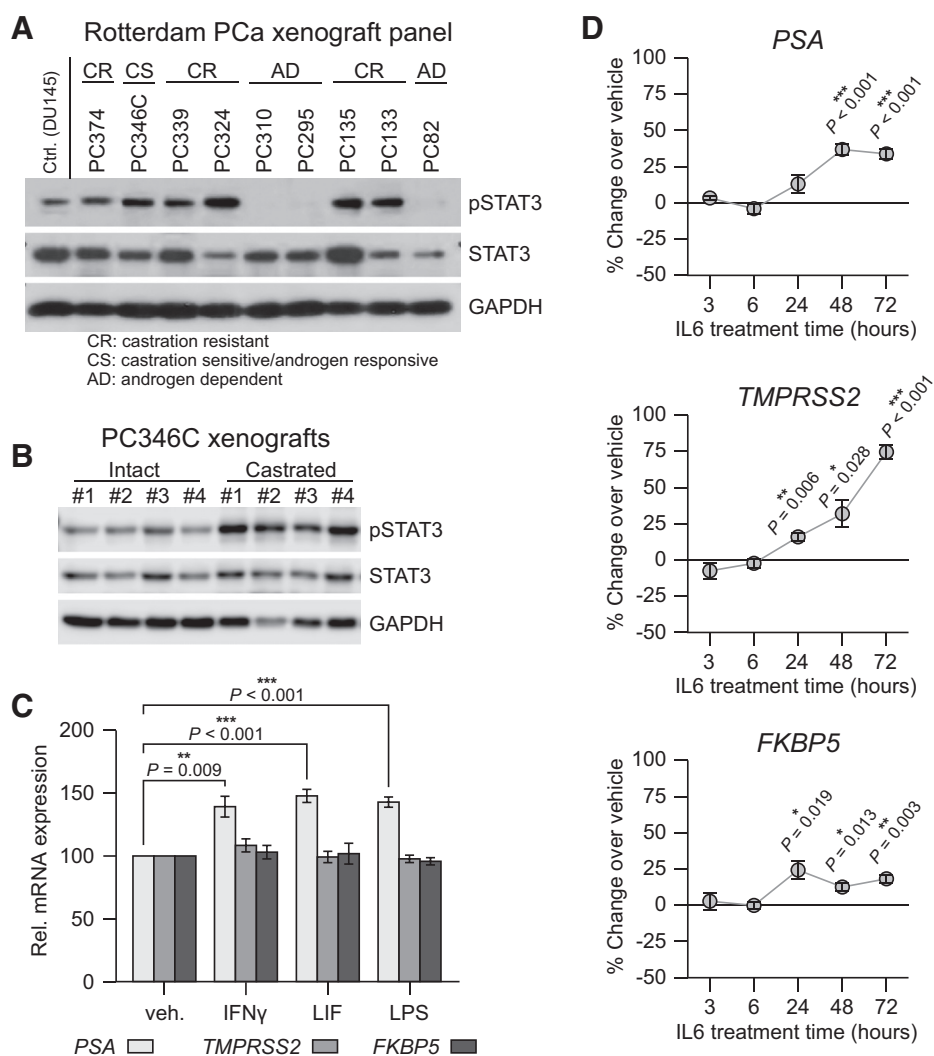


Figure 3.

STAT3 is highly activated in castration-resistant xenografts and acts on AR activity in an indirect manner. **A**, STAT3 activity in castration-resistant (CR), castration-sensitive/androgen-responsive (CS), and androgen-dependent (AD) prostate cancer (PCa) xenografts. **B**, Activation of STAT3 in PC346C xenografts upon castration. **C**, LNCaP cells were treated with IFN-gamma (10 ng/mL), LIF (10 ng/mL), and LPS (10 μ g/mL) for 72 hours, and the effect on AR activity was measured by RT-qPCR. **D**, LNCaP cells were equilibrated in steroid-depleted medium supplemented with 1 nmol/L R1881 for 48 hours before treatment with and without 10 ng/mL IL6. The cells were harvested at each given time point, and IL6-induced AR activity was measured by RT-qPCR on the AR target genes PSA, TMPRSS2, and FKBP5 by comparing the IL6-treated cells with the untreated controls.

FKBP5 after treatment with the other STAT3 activators. Taken together, STAT3 is highly activated in castration-resistant xenografts, and multiple STAT3 activating cytokines can increase AR activity at least partially.

IL6-dependent AR activation is slower than canonical androgen-mediated activation

In order to understand how STAT3 influences AR signaling, we performed time-course experiments. Canonical activation of the AR (by R1881) and STAT3 (by IL6) are rapid processes, given that their respective transcriptional target genes are induced within 3 to 6 hours (Supplementary Fig. S1B). However, we do not have any information so far whether IL6 is able to influence AR activity with a similar kinetic profile. To exclude androgen and cell density-dependent effects LNCaP cells were adapted to a high androgen concentration (1 nmol/L R1881) for 48 hours and each time point was normalized to the control well without IL6. In contrast to R1881-mediated AR activity, we did not observe an IL6-dependent induction of AR activity at 3 to 6 hours (Fig. 3D). Of note, AR activation by IL6 required at least 24 hours, and the maximum effect was seen after 48 to 72 hours for PSA and TMPRSS2. Interestingly, the kinetic profile of FKBP5 activation was slightly

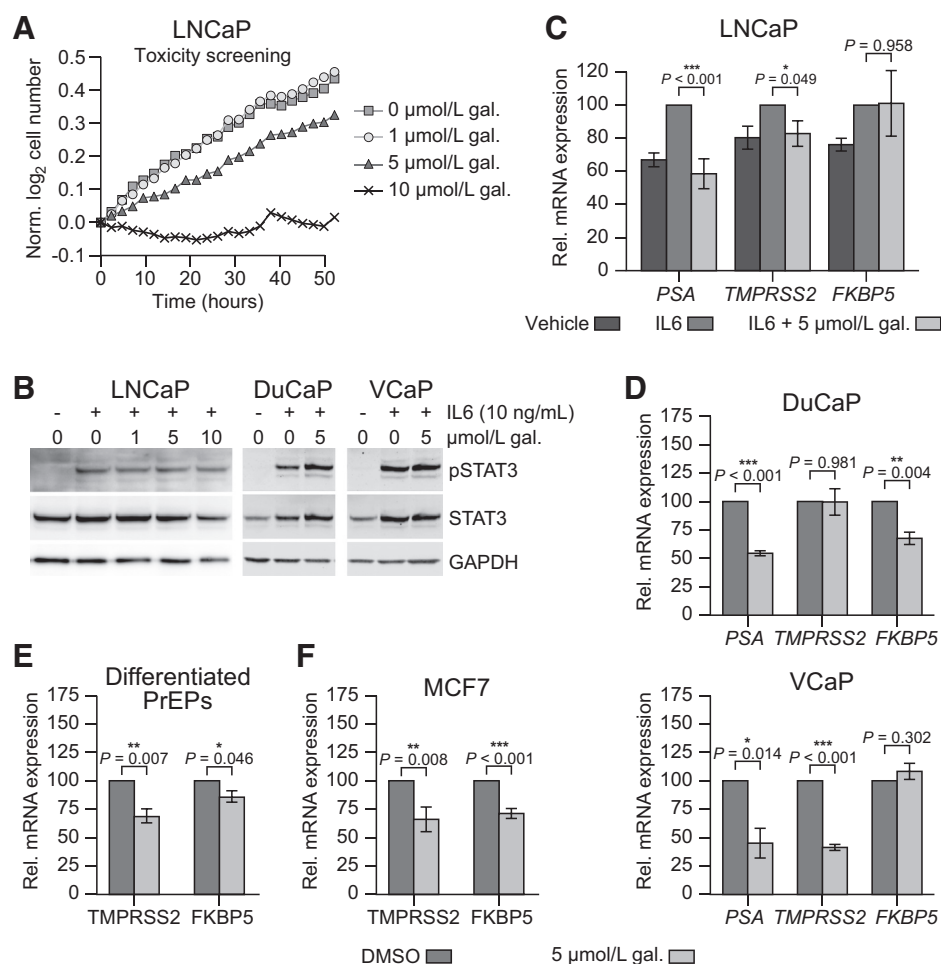
different, and no further increases were seen after 24 hours. This finding indicates that the effect of IL6 on AR activity is most likely an indirect one, involving a more complex and thus time-consuming mechanism (i.e., chromatin remodeling or induction of STAT3 target genes that subsequently influence AR activity). Thus, inhibition of the transcriptional activity of STAT3 may be a promising approach to block IL6-induced AR activity.

Inhibition of the STAT3 DNA-binding domain with galiellalactone reduces AR activity

On the basis of the time-course experiment, we wanted to test whether a STAT3-DNA interaction is required for IL6-dependent AR activity. To this end, we decided to use the small-molecule inhibitor galiellalactone because it irreversibly inactivates the STAT3 DNA-binding domain without decreasing STAT3 phosphorylation (35). To identify the maximum concentration that is tolerated by the cells, we treated LNCaP cells with 1 to 10 μ mol/L galiellalactone in the presence of 10 ng/mL IL6 and 1 nmol/L R1881 (Fig. 4A). Because LNCaP cells were able to grow in the presence of 5 μ mol/L galiellalactone (albeit at a slightly reduced rate), we selected this concentration for all further experiments. At this concentration, galiellalactone efficiently reduced expression

Figure 4.

Inhibition of the STAT3 DNA-binding domain with galiellalactone reduces AR activity. **A**, The effect of the STAT3 inhibitor galiellalactone on LNCaP proliferation in the presence of 10 ng/mL IL6 was measured with the InCuCyte life cell imaging system. **B**, Multiple AR-positive cell lines were treated with galiellalactone for 72 hours in the presence of 10 ng/mL IL6, and the effect on phosphorylation and total expression of STAT3 was evaluated by Western blotting. **C** and **D**, The prostate cancer cell lines LNCaP, DuCaP, and VCaP were treated with 5 μ mol/L galiellalactone for 72 hours in the presence of 1 nmol/L R1881 and 10 ng/mL IL6 before measurement of AR activity. **E**, Benign primary epithelial cells (PrEP) were differentiated into a more luminal phenotype for 7 days. The differentiated PrEPs were treated with 5 μ mol/L galiellalactone for 72 hours in the presence of 1 nmol/L R1881 and 10 ng/mL IL6 before measurement of AR activity. **F**, The AR-positive breast cancer cell line MCF7 was treated with 5 μ mol/L galiellalactone for 72 hours in the presence of 10 nmol/L DHT and 10 ng/mL IL6 before measurement of AR activity.



of the STAT3 target gene SOCS3 in the presence of 10 ng/mL IL6 (Supplementary Fig. S2) without reducing STAT3 phosphorylation (Fig. 4B). Galiellalactone treatment completely inhibited the effect of IL6 on the expression of the AR target genes PSA and TMPRSS2 but surprisingly did not influence FKBP5 expression (Fig. 4C). To confirm the effect of galiellalactone in other AR-positive cell lines and primary patient material, we treated the prostate cancer cell lines DuCaP and VCaP (Fig. 4D) and differentiated benign prostate basal epithelial cells (PrEP; Fig. 4E). Because AR inhibition is currently evaluated in clinical trials for certain breast cancer subtypes, we also included the AR-positive breast cancer cell line MCF7 (Fig. 4F). Expression of the AR target genes was significantly reduced in all cell lines, albeit *TMPRSS2* in DuCaP and *FKBP5* in VCaP cells remained unaffected by galiellalactone treatment. Because the GR is known to activate AR target genes in certain conditions and activated STAT3 increases also the transcriptional activity of the GR (34, 36), we were interested whether this may explain the differential response between the cell lines and target genes. However, in LNCaP, DuCaP, and VCaP cells we only observed minimal *GR* mRNA expression levels. In contrast, MCF7 cells and undifferentiated PrEPs had detectable levels of *GR* mRNA (Supplementary Fig. S3). On protein level, we have previously shown that *GR* expression is very low in LNCaP, DuCaP, and VCaP cells compared with DU145 (37). Therefore, it is unlikely that the *GR* influences the AR target genes in LNCaP,

DuCaP, and VCaP cells, but it may contribute to the effects seen in PrEPs and MCF7 cells. Taken together, this demonstrates that inhibiting the DNA-binding domain of STAT3 with galiellalactone reduces AR activity on a subset of AR target genes in the presence of IL6 and androgens.

Galiellalactone reduces AR activity in benign and a subset of cancerous prostate tissue samples in an *ex vivo* culture model

On the basis of the results obtained with cell lines, we next aimed to determine whether galiellalactone is able to reduce AR activity within the natural microenvironment of living prostate tissue samples. To this end, we prepared approximately 0.5-mm thin slices from cancerous and adjacent benign tissue cores from treatment-naïve radical prostatectomy patients. Correct assignment of the tissue biopsy samples was verified by an expert uropathologist. Although *ex vivo* tissue slice cultures have been shown to maintain viability and proper luminal tissue architecture for up to 7 days (38), we decided to restrict the cultivation to the same timeframe (72 hours) used in the cell culture experiments. A schematic overview of the procedure is shown in Fig. 5A. All samples were treated with 5 μ mol/L galiellalactone or vehicle in the presence of 10 nmol/L DHT and 5 ng/mL IL6. Of note, galiellalactone treatment strongly reduced the expression of *PSA* (\log_2 fold change >1) in more than 50% of the benign samples (Fig. 5B; Supplementary

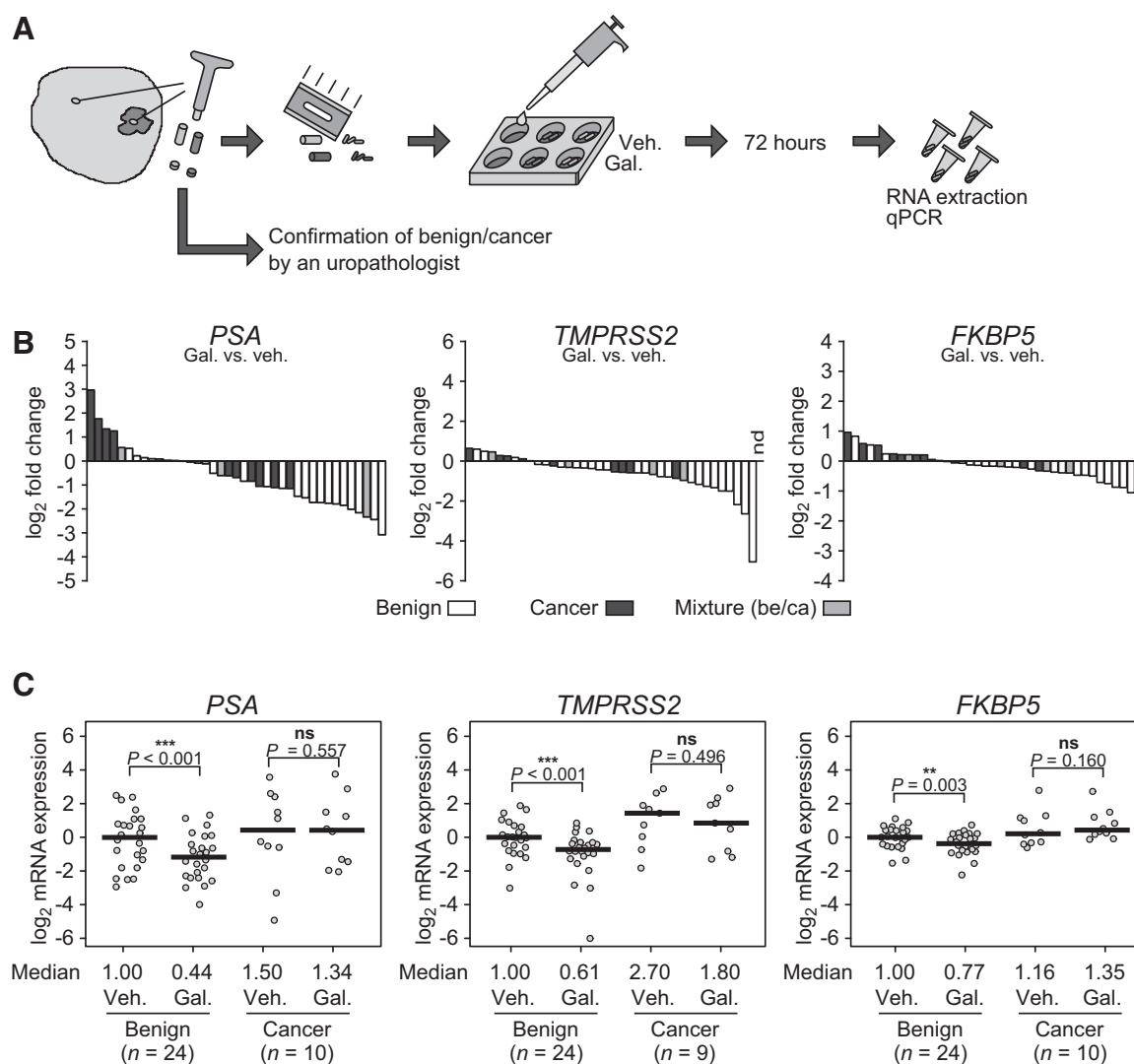


Figure 5. Galiellalactone reduces AR activity in benign and a subset of cancerous *ex vivo* prostate tissue cultures. **A**, Small tissue samples were prepared from freshly explanted prostates of prostate cancer patients undergoing radical prostatectomy and cut into thin slices. The tissue slices were incubated at the air-liquid interface in multiwell plates and treated with and without 5 $\mu\text{mol/L}$ galiellalactone for 72 hours in the presence of 10 nmol/L DHT and 5 ng/mL IL6. Expression of the AR target genes *PSA*, *TMPRSS2*, and *FKBP5* was measured by RT-qPCR. **B**, Waterfall plots of the galiellalactone induced \log_2 fold change in all samples. **C**, Relative mRNA expression of the tested AR target genes in the confirmed benign and cancerous samples.

Fig. S4). Statistical paired sample analysis revealed that the expression of all tested AR target genes was significantly reduced by galiellalactone in benign tissues. Median expression was reduced by 56% (*PSA*), 39% (*TMPRSS2*), and 23% (*FKBP5*), respectively (Fig. 5C). Interestingly, we observed that galiellalactone treatment resulted in a much more heterogeneous response in the cancerous tissue samples. Specifically, *PSA* expression ($n = 10$) was increased in 3 samples and decreased in 4 samples upon galiellalactone treatment (\log_2 fold change >1). Response to galiellalactone was not related to *PSA* expression level (Supplementary Fig. S4). Expression levels of AR and the luminal marker *KRT8* were mostly unchanged by galiellalactone treatment, although we observed a small reduction in benign tissue samples (Supplementary Fig. S4).

Discussion

IL6 signaling in prostate cancer and, more specifically, IL6-mediated AR activity have been intensively investigated by many research groups in the past. IL6 is known to regulate proliferation, apoptosis, neuroendocrine differentiation, and epithelial-to-mesenchymal transition in prostate cancer cells (6). However, the resulting knowledge has not been translated into clinical practice for the treatment of prostate cancer so far, and several attempts to develop anti-IL6 therapies have failed in clinical trials (12, 19, 20). This fact clearly demonstrates that our current understanding of the IL6 pathway and its interaction with AR signaling is not sufficient to identify susceptible tumor stages and patient subpopulations for novel (combination) treatment strategies.

Endocrine therapy is the gold standard for treatment of advanced prostate cancer. Therefore, it is of particular note that IL6 has been proposed to induce AR activity in the absence of androgens, as well as in the presence of androgenic hormones (11, 30–32, 39). On the basis of these findings, IL6 has been implicated in resistance to androgen deprivation therapy. However, inhibition of the IL6 pathway with siltuximab (anti-IL6) and ruxolitinib (anti-JAK1/2) did not show any clinical benefit in clinical trials in CRPC patients (12, 19, 20).

In the present study, we confirmed that IL6 increases the transactivation potential of the AR; however, this effect was observed only in the presence of moderate to high androgen concentrations. In particular, we did not observe any IL6-mediated AR activation at 1 to 10 pmol/L of R1881, which is biologically comparable with castrate testosterone levels found in patients, considering the 10- to 100-fold higher transactivation capacity of R1881 (40, 41). This is in contrast to several previous publications that have found androgen-independent effects of IL6 on AR activity. Importantly, however, these studies have also confirmed an IL6-mediated increase in the hormone-dependent response (11, 42). Similar to our results, De Miguel and colleagues has previously reported that active STAT3 enhances AR activity exclusively in a hormone-dependent manner (34). The fact that we could not reproduce the androgen-independent effects of IL6 on AR activity may be explained by variations in the concentration of residual androgens in the steroid-depleted serum and different experimental procedures. In previous publications, the effect of IL6 on AR activity was predominantly measured by reporter gene assays using short androgen response elements. In contrast, we measured AR activity on three natural target genes by RT-qPCR, which enables us to evaluate the complex nature of gene regulation on natural chromatin. Therefore, chromatin remodeling or distant enhancers may play an important role in the regulation of IL6-mediated AR activity. Taken together, our results indicate that anti-IL6 therapies may have the strongest effect on AR activity in patients with high intratumoral levels of androgens. Considering that intratumoral production of androgens is frequently found in CRPC patients (43) and that IL6 has been proposed to induce the expression of genes responsible for androgen synthesis (44), all further experiments were carried out in the presence of high androgen concentrations.

To ensure specific inhibition of IL6-mediated AR activity, we first wanted to narrow down which pathways are influenced by IL6. The effect of IL6 on AR signaling has been associated with different downstream signaling pathways (STAT3, MAPK, and PI3K) in the literature (30, 33, 42). Our results confirmed that IL6 influences its canonical downstream mediator STAT3 in LNCaP cells, but we did not observe any IL6-dependent changes in MAPK and PI3K signaling in our particular setting. However, these pathways may contribute to IL6-dependent AR activity under certain conditions because IL6 directly influences these pathways in other cell lines and MAPK/PI3K signaling are both well known to regulate AR activity (45). Nevertheless, we decided to focus on STAT3 signaling in the present study because STAT3 plays an important role in advanced prostate cancer, and 95% of metastatic samples from CRPC patients were found to be positive for activated STAT3 (9). Our experiments confirmed high STAT3 activation in CRPC xenografts and that STAT3 phosphorylation was increased upon castration in hormone-sensitive prostate cancer xenografts. Interestingly, we observed that other known inducers of STAT3 phosphorylation are able to increase the

expression of PSA but not of *TMPRSS2* and *FKBP5*, which may be due to the additional activation of other signaling pathways, such as MAPK and PI3K/AKT. Mechanistically, activated STAT3 has been proposed to increase AR activity by direct physical interaction with the N-terminal region of the AR (30, 46). To identify which domain of STAT3 is responsible for mediating the effect of IL6 on AR activity, we performed time-course experiments. AR and STAT3 are both activated within 30 to 60 minutes after the addition of their respective canonical agonists (47, 48), but the effect of IL6 on AR activity was much slower. This indicates that regulation of AR activity by IL6 is most likely controlled by an indirect mechanism. Of note, the histone acetyltransferase activity of p300 has been implicated in IL6-dependent activation of AR, and p300 is known to bind STAT3 upon IL6 stimulation (49). This may lead to chromatin remodeling either due to AR/STAT3 protein–protein interaction or due to direct DNA binding of STAT3 close to AR target genes. However, it is also possible that a transcriptional target gene of STAT3 is responsible for the increase in AR activity upon IL6 treatment. Interestingly, STAT3 is known to induce its own expression in a positive feedback loop (50), and we observed an increase in total STAT3 levels upon IL6 treatment. This feedback induction might stabilize the reported physical interaction between AR and STAT3 and thus enhance AR activity. On the basis of the time-course results, we decided to test whether inhibition of the STAT3 DNA-binding domain with galiellalactone leads to a reduction in AR activity in the presence of IL6.

Galiellalactone was able to reduce tumor growth as well as metastatic spread of an AR-negative prostate cancer cell line in xenograft models (13) and inhibited the growth of triple-negative breast cancer cell lines (15). Recently, an orally available prodrug of galiellalactone has been described (51). However, galiellalactone has not yet been tested in the context of AR signaling. To ensure that galiellalactone consistently reduces AR activity, we selected several AR-positive prostate cancer cell lines and benign primary epithelial prostate cells. In addition, we also included one AR-positive breast cancer cell line. Galiellalactone significantly reduced AR activity in the presence of IL6 in all tested cell lines. Interestingly, we observed differences in the response of the individual AR target genes, which may influence the physiologic response of the cells. It is noteworthy that *FKBP5*, which was unaffected by inhibition of the STAT3 DNA-binding domain in LNCaP, also showed a different kinetic profile in the time-course experiment. It is therefore possible that STAT3 influences AR activity by various means, some of which require DNA binding (i.e., induction of AR coactivators), whereas others are independent of a direct STAT3–DNA interaction (i.e., chromatin remodeling due to AR/STAT3 protein–protein interaction). However, induction of *PSA* and *TMPRSS2* was completely inhibited by galiellalactone in LNCaP cells, which demonstrates the importance of the STAT3 DNA-binding domain. In addition, we observed variations between VCaP and DuCaP cells. Although these cell lines were obtained from the same patient, they represent two different metastatic lesions. In line with this, analysis of publicly available transcriptome data (27) from VCaP and DuCaP cells confirms that a large number genes are significantly deregulated between both cell lines (Supplementary Fig. S5). Therefore, differences in the expression of pioneering factors or AR coregulators may explain their individual response to galiellalactone. Furthermore, other nuclear hormone receptors may also be influenced by IL6. Especially, the GR is known to activate AR target

genes in certain conditions (36), and we found GR mRNA expression in PrEPs and MCF7 cells. However, based on its expression level, we can rule out that the GR is responsible for the variations in AR target gene response seen in LNCaP, VCaP, and DuCaP cells. Taken together, we conclude that the small-molecule inhibitor galiellalactone is a promising drug to reduce AR activity in the presence of IL6 and androgens.

Because several clinical trials targeting the IL6 pathway have failed despite very promising preclinical results in cell culture and xenograft experiments (12, 19, 20), we aimed to verify our cell culture experiments in primary patient material. To this end, we tested the effect of galiellalactone in the presence of IL6 in an innovative *ex vivo* tissue slice culture model with material from patients undergoing radical prostatectomy. In benign tissue samples, the results were very well in line with our *in vitro* findings and galiellalactone significantly reduced the expression of the tested AR target genes. Surprisingly, we observed a very heterogeneous response to galiellalactone in cancerous samples, and PSA expression was increased in some and decreased in other tissue samples. Although we cannot fully explain this variability in response to galiellalactone, we suspect that a difference in the AR coactivator profile may cause a shift in the interplay of STAT3/AR signaling. Specifically, the complex interaction of cancer cells with their surrounding tumor microenvironment may play an important role in determining the effect of STAT3 on AR activity. The pleiotropic role of IL6/STAT3 signaling has been published in the past, and recently STAT3 has been reported to act as a tumor suppressor in a *PTEN* knockout mouse model (52). These findings might shed some light on the reason why inhibitors targeting the IL6 pathway have failed in clinical trials despite very promising cell culture results. However, the low number of confirmed cancer samples is a limitation of this study, and additional confirmation studies are therefore required in the future.

Taken together, we demonstrated that the STAT3 inhibitor galiellalactone consistently reduces IL6-mediated AR activity in cancer cell lines and benign prostate tissue cultures, as well as in a subgroup of malignant tissue cultures in the presence of androgens. On the basis of this finding, we propose that follow-up studies should focus on identifying a biomarker that predicts the

response to IL6/STAT3 inhibition before future clinical trials targeting this pathway are initiated.

Disclosure of Potential Conflicts of Interest

Z. Culig reports receiving a commercial research grant from and has received honoraria from the speakers bureau of Astellas. No potential conflicts of interest were disclosed by the other authors.

Authors' Contributions

Conception and design: F. Handle, H.H.H. Erb, Z. Culig

Development of methodology: F. Handle, M. Puhr, G. Schaefer, F.R. Santer, H.H.H. Erb

Acquisition of data (provided animals, acquired and managed patients, provided facilities, etc.): F. Handle, M. Puhr, N. Lorito, J. Hoefler, M. Gruber, R.B. Marques, W.M. van Weerden, F. Claessens

Analysis and interpretation of data (e.g., statistical analysis, biostatistics, computational analysis): F. Handle, M. Puhr, N. Lorito, W.M. van Weerden, H.H.H. Erb, Z. Culig

Writing, review, and/or revision of the manuscript: F. Handle, M. Puhr, G. Schaefer, M. Gruber, F. Guggenberger, F.R. Santer, R.B. Marques, W.M. van Weerden, F. Claessens, H.H.H. Erb, Z. Culig

Administrative, technical, or material support (i.e., reporting or organizing data, constructing databases): G. Schaefer, M. Gruber, H.H.H. Erb

Study supervision: Z. Culig

Other (isolation and cultivation of primary human prostate cells used in this study): F. Guggenberger

Acknowledgments

The authors thank Sarah Peer and Gabriele Dobler for their help with the *ex vivo* tissue culture experiments, Dr. Georg Grünbacher and Dr. Martin Thurnher for providing us with the LPS, Dr. Walther Parson for cell authentication, and all members of the Division of Experimental Urology at the Medical University of Innsbruck and the Molecular Endocrinology Laboratory at the KU Leuven for helpful discussions. This work was supported by grants from the Austrian Cancer Society/Tirol (to F. Handle) and the Austrian Science Fund (FWF) W1101-B12 (to Z. Culig).

The costs of publication of this article were defrayed in part by the payment of page charges. This article must therefore be hereby marked *advertisement* in accordance with 18 U.S.C. Section 1734 solely to indicate this fact.

Received May 20, 2018; revised August 23, 2018; accepted September 20, 2018; published first September 25, 2018.

References

- Katzenwadel A, Wolf P. Androgen deprivation of prostate cancer: leading to a therapeutic dead end. *Cancer Lett* 2015;367:12–7.
- Culig Z, Santer FR. Androgen receptor signaling in prostate cancer. *Cancer Metastasis Rev* 2014;33:413–27.
- Scher HI, Fizazi K, Saad F, Taplin ME, Sternberg CN, Miller K, et al. Increased survival with enzalutamide in prostate cancer after chemotherapy. *N Engl J Med* 2012;367:1187–97.
- Beer TM, Armstrong AJ, Rathkopf DE, Loriot Y, Sternberg CN, Higano CS, et al. Enzalutamide in metastatic prostate cancer before chemotherapy. *N Engl J Med* 2014;371:424–33.
- Yu SH, Zheng Q, Esopi D, Macgregor-Das A, Luo J, Antonarakis ES, et al. A paracrine role for IL6 in prostate cancer patients: lack of production by primary or metastatic tumor cells. *Cancer Immunol Res* 2015;3:1175–84.
- Culig Z. Proinflammatory cytokine interleukin-6 in prostate carcinogenesis. *Am J Clin Exp Urol* 2014;2:231–8.
- Lee SO, Lou W, Hou M, de Miguel F, Gerber L, Gao AC. Interleukin-6 promotes androgen-independent growth in LNCaP human prostate cancer cells. *Clin Cancer Res* 2003;9:370–6.
- Shariat SF, Karam JA, Walz J, Roehrborn CG, Montorsi F, Margulis V, et al. Improved prediction of disease relapse after radical prostatectomy through a panel of preoperative blood-based biomarkers. *Clin Cancer Res* 2008;14:3785–91.
- Don-Doncow N, Marginean F, Coleman I, Nelson PS, Ehrnström R, Krzyzanowska A, et al. Expression of STAT3 in prostate cancer metastases. *Eur Urol* 2017;71:313–6.
- Handle F, Erb HH, Luef B, Hoefler J, Dietrich D, Parson W, et al. SOCS3 modulates the response to enzalutamide and is regulated by androgen receptor signaling and CpG methylation in prostate cancer cells. *Mol Cancer Res* 2016;14:574–85.
- Hobisch A, Eder IE, Putz T, Horninger W, Bartsch G, Klocker H, et al. Interleukin-6 regulates prostate-specific protein expression in prostate carcinoma cells by activation of the androgen receptor. *Cancer Res* 1998;58:4640–5.
- Culig Z, Puhr M. Interleukin-6 and prostate cancer: current developments and unsolved questions. *Mol Cell Endocrinol* 2018;462:25–30.
- Canesin G, Evans-Axelsson S, Hellsten R, Sterner O, Krzyzanowska A, Andersson T, et al. The STAT3 inhibitor galiellalactone effectively reduces tumor growth and metastatic spread in an orthotopic xenograft mouse model of prostate cancer. *Eur Urol* 2016;69:400–4.

14. Hellsten R, Johansson M, Dahlgren A, Sterner O, Bjartell A. Galiellalactone inhibits stem cell-like ALDH-positive prostate cancer cells. *PLoS One* 2011;6:e22118.
15. Kim HS, Kim T, Ko H, Lee J, Kim YS, Suh YG. Identification of galiellalactone-based novel STAT3-selective inhibitors with cytotoxic activities against triple-negative breast cancer cell lines. *Bioorg Med Chem* 2017; 25:5032–40.
16. Steiner H, Cavarretta IT, Moser PL, Berger AP, Bektic J, Dietrich H, et al. Regulation of growth of prostate cancer cells selected in the presence of interleukin-6 by the anti-interleukin-6 antibody CNTO 328. *Prostate* 2006;66:1744–52.
17. Erb HH, Langlechner RV, Moser PL, Handle F, Casneuf T, Verstraeten K, et al. IL6 sensitizes prostate cancer to the antiproliferative effect of IFN α 2 through IRF9. *Endocr Relat Cancer* 2013;20:677–89.
18. Chen R, Chen B. Siltuximab (CNTO 328): a promising option for human malignancies. *Drug Des Devel Ther* 2015;9:3455–8.
19. Dorff TB, Goldman B, Pinski JK, Mack PC, Lara PN, Van Veldhuizen PJ, et al. Clinical and correlative results of SWOG S0354: a phase II trial of CNTO328 (siltuximab), a monoclonal antibody against interleukin-6, in chemotherapy-pretreated patients with castration-resistant prostate cancer. *Clin Cancer Res* 2010;16:3028–34.
20. Fizazi K, De Bono JS, Flechon A, Heidenreich A, Voog E, Davis NB, et al. Randomised phase II study of siltuximab (CNTO 328), an anti-IL-6 monoclonal antibody, in combination with mitoxantrone/prednisone versus mitoxantrone/prednisone alone in metastatic castration-resistant prostate cancer. *Eur J Cancer* 2012;48:85–93.
21. Santer FR, Erb HH, Oh SJ, Handle F, Feiersinger GE, Luef B, et al. Mechanistic rationale for MCL1 inhibition during androgen deprivation therapy. *Oncotarget* 2015;6:6105–22.
22. van Weerden WM, de Ridder CM, Verdaasdonk CL, Romijn JC, van der Kwast TH, Schröder FH, et al. Development of seven new human prostate tumor xenograft models and their histopathological characterization. *Am J Pathol* 1996;149:1055–62.
23. Marques RB, van Weerden WM, Erkens-Schulze S, de Ridder CM, Bangma CH, Trapman J, et al. The human PC346 xenograft and cell line panel: a model system for prostate cancer progression. *Eur Urol* 2006;49:245–57.
24. Marques RB, Aghai A, de Ridder CM, Stuurman D, Hoeben S, Boer A, et al. High efficacy of combination therapy using PI3K/AKT inhibitors with androgen deprivation in prostate cancer preclinical models. *Eur Urol* 2015;67:1177–85.
25. Wang XD, Reeves K, Luo FR, Xu LA, Lee F, Clark E, et al. Identification of candidate predictive and surrogate molecular markers for dasatinib in prostate cancer: rationale for patient selection and efficacy monitoring. *Genome Biol* 2007;8:R255.
26. Hook KE, Garza SJ, Lira ME, Ching KA, Lee NV, Cao J, et al. An integrated genomic approach to identify predictive biomarkers of response to the aurora kinase inhibitor PF-03814735. *Mol Cancer Ther* 2012;11:710–9.
27. Hoefler J, Kern J, Ofer P, Eder IE, Schäfer G, Dietrich D, et al. SOCS2 correlates with malignancy and exerts growth-promoting effects in prostate cancer. *Endocr Relat Cancer* 2014;21:175–87.
28. Barretina J, Caponigro G, Stransky N, Venkatesan K, Margolin AA, Kim S, et al. The Cancer Cell Line Encyclopedia enables predictive modelling of anticancer drug sensitivity. *Nature* 2012;483:603–7.
29. Guggenberger F, van de Werken HJG, Erb HHH, Cappellano G, Trattng K, Handle F, et al. Fractionated radiation of primary prostate basal cells results in downplay of interferon stem cell and cell cycle checkpoint signatures. *Eur Urol* 2018. pii: S0302-2838(18)30427-5.
30. Ueda T, Bruchovsky N, Sadar MD. Activation of the androgen receptor N-terminal domain by interleukin-6 via MAPK and STAT3 signal transduction pathways. *J Biol Chem* 2002;277:7076–85.
31. Chen T, Wang LH, Farrar WL. Interleukin 6 activates androgen receptor-mediated gene expression through a signal transducer and activator of transcription 3-dependent pathway in LNCaP prostate cancer cells. *Cancer Res* 2000;60:2132–5.
32. Lin DL, Whitney MC, Yao Z, Keller ET. Interleukin-6 induces androgen responsiveness in prostate cancer cells through up-regulation of androgen receptor expression. *Clin Cancer Res* 2001;7:1773–81.
33. Yang L, Wang L, Lin HK, Kan PY, Xie S, Tsai MY, et al. Interleukin-6 differentially regulates androgen receptor transactivation via PI3K-Akt, STAT3, and MAPK, three distinct signal pathways in prostate cancer cells. *Biochem Biophys Res Commun* 2003;305:462–9.
34. De Miguel F, Lee SO, Onate SA, Gao AC. Stat3 enhances transactivation of steroid hormone receptors. *Nucl Recept* 2003;1:3.
35. Don-Doncow N, Escobar Z, Johansson M, Kjellström S, Garcia V, Munoz E, et al. Galiellalactone is a direct inhibitor of the transcription factor STAT3 in prostate cancer cells. *J Biol Chem* 2014;289:15969–78.
36. Arora VK, Schenkein E, Murali R, Subudhi SK, Wongvipat J, Balbas MD, et al. Glucocorticoid receptor confers resistance to antiandrogens by bypassing androgen receptor blockade. *Cell* 2013;155:1309–22.
37. Puhm M, Hoefler J, Eigentler A, Ploner C, Handle F, Schaefer G, et al. The glucocorticoid receptor is a key player for prostate cancer cell survival and a target for improved anti-androgen therapy. *Clin Cancer Res* 2018;24:927–38.
38. Maund SL, Nolley R, Peehl DM. Optimization and comprehensive characterization of a faithful tissue culture model of the benign and malignant human prostate. *Lab Invest* 2014;94:208–21.
39. Kim O, Jiang T, Xie Y, Guo Z, Chen H, Qiu Y. Synergism of cytoplasmic kinases in IL6-induced ligand-independent activation of androgen receptor in prostate cancer cells. *Oncogene* 2004;23:1838–44.
40. Nishiyama T. Serum testosterone levels after medical or surgical androgen deprivation: a comprehensive review of the literature. *Urol Oncol* 2014;32:38.e17–28.
41. Kleinstreuer NC, Ceger P, Watt ED, Martin M, Houck K, Browne P, et al. Development and validation of a computational model for androgen receptor activity. *Chem Res Toxicol* 2017;30:946–64.
42. Ueda T, Mawji NR, Bruchovsky N, Sadar MD. Ligand-independent activation of the androgen receptor by interleukin-6 and the role of steroid receptor coactivator-1 in prostate cancer cells. *J Biol Chem* 2002;277: 38087–94.
43. Montgomery RB, Mostaghel EA, Vessella R, Hess DL, Kalhorn TF, Higano CS, et al. Maintenance of intratumoral androgens in metastatic prostate cancer: a mechanism for castration-resistant tumor growth. *Cancer Res* 2008;68:4447–54.
44. Chun JY, Nadiminty N, Dutt S, Lou W, Yang JC, Kung HJ, et al. Interleukin-6 regulates androgen synthesis in prostate cancer cells. *Clin Cancer Res* 2009;15:4815–22.
45. Eulenfeld R, Dittrich A, Khouri C, Müller PJ, Mütze B, Wolf A, et al. Interleukin-6 signalling: more than Jaks and STATs. *Eur J Cell Biol* 2012; 91:486–95.
46. Matsuda T, Junicho A, Yamamoto T, Kishi H, Korkmaz K, Saatcioglu F, et al. Cross-talk between signal transducer and activator of transcription 3 and androgen receptor signaling in prostate carcinoma cells. *Biochem Biophys Res Commun* 2001;283:179–87.
47. Georget V, Lobaccaro JM, Terouanne B, Mangeat P, Nicolas JC, Sultan C. Trafficking of the androgen receptor in living cells with fused green fluorescent protein-androgen receptor. *Mol Cell Endocrinol* 1997;129: 17–26.
48. Liu L, McBride KM, Reich NC. STAT3 nuclear import is independent of tyrosine phosphorylation and mediated by importin- α 3. *Proc Natl Acad Sci U S A* 2005;102:8150–5.
49. Debes JD, Schmidt LJ, Huang H, Tindall DJ. p300 mediates androgen-independent transactivation of the androgen receptor by interleukin 6. *Cancer Res* 2002;62:5632–6.
50. Ichiba M, Nakajima K, Yamanaka Y, Kiuchi N, Hirano T. Autoregulation of the Stat3 gene through cooperation with a cAMP-responsive element-binding protein. *J Biol Chem* 1998;273:6132–8.
51. Escobar Z, Bjartell A, Canesin G, Evans-Axelsson S, Sterner O, Hellsten R, et al. Preclinical Characterization of 3 β -(N-Acetyl L-cysteine methyl ester)-2 α ,3-dihydrogaliellalactone (GPA512), a prodrug of a direct STAT3 inhibitor for the treatment of prostate cancer. *J Med Chem* 2016;59: 4551–62.
52. Pencik J, Schleder M, Gruber W, Unger C, Walker SM, Chalaris A, et al. STAT3 regulated ARF expression suppresses prostate cancer metastasis. *Nat Commun* 2015;6:7736.